Desalination and Water Treatment
www.deswater.com

doi: 10.1080/19443994.2015.1132476

57 (2016) 22573–22584
October

Taylor & Francis
Taylor & Francis Group

Adsorption of methylene blue by activated carbon derived from various fruit peels

F.S. Hashem[b], M.S. Amin[a,b,*]

[a]*Department of Basic Sciences and Technology, Community College, Taibah University, Almadina almonawara, Saudi Arabia, Tel. +20 1001648958; email: mohamedsamin@hotmail.com (M.S. Amin)*
[b]*Faculty of Science, Chemistry Department, Ain Shams University, Abbassia, Cairo, Egypt, Tel. +966 563526533; email: f_s_hashem@yahoo.com (F.S. Hashem)*

Received 11 April 2015; Accepted 11 December 2015

ABSTRACT

In this study, activated carbon (AC) derived from orange, mandarin, and banana peels has been utilized as an adsorbent for the removal of a cationic dye, methylene blue, from aqueous solutions. The batch adsorption technique was used with these materials under different conditions of contact time, initial dye concentration (10–100 mg/L), solution pH (4–12), and AC dosage (0.05–0.5 g). The characteristics of the prepared ACs were studied via FTIR, mercury porosimetry, and iodine number determination. Banana peels showed the highest removal efficiency compared with the other fruit peels. Adsorption isotherms were modeled with the Langmuir and Freundlich isotherms, and good fitting to the Freundlich isotherm was obtained. The kinetic data were analyzed using pseudo-first-order, second-order, and intraparticles diffusion models, with good fitting to the pseudo-second-order model. The obtained results indicate that AC represents an efficient low-cost adsorbent for the removal of MB from aqueous solutions.

Keywords: Adsorption isotherm; Fruit peels; Methylene blue; Activated carbon; Adsorption kinetics

1. Introduction

Dyes are organic compounds that can bring bright and strong colors to other substances. Synthetic dyes usually have complex aromatic molecular structures, which possibly come from coal tar-based hydrocarbons, such as benzene, naphthalene, anthracene, toluene, and xylene. These complex aromatic molecular structures make them more stable and more difficult to biodegrade [1,2]. There are more than 10,000 commercially available dyes [3]. The discharge of dyes into rivers, groundwater systems, and other water sources represents a serious pollution problem. Color is considered a primary indicator of contaminants in wastewater because even a very small amount of dye in water is highly visible and undesirable. Dyes are designed to resist breakdown when they are exposed to sunlight, water, soap, and oxidizing agents, so they cannot be easily removed by conventional wastewater treatment processes.

Several technologies have been developed for dyed wastewater treatment, including oxidation, photocatalytic degradation [4], micellar-enhanced ultrafiltration [5], adsorption/precipitation processes [6], and coagulation. Of all these technologies, adsorption represents a simple and economical technique that has recently

*Corresponding author.

been used with success [7–9]. In the adsorption process, certain solids serve as adsorbents, which are able to concentrate specific substances from the liquid phase onto their surfaces. Most of the known adsorbents are available at low cost, but they have some disadvantages, such as a relatively limited adsorption capacity for dyes. An economic adsorbent is defined as one that is abundant in nature or is a by-product of industry and requires little processing. Many researchers have considered low cost and effective substitutes, such as waste metals, coconut husks [10], spent tea leaves [11], fly ash [12–15], banana peels [5], peanut hulls [16], peach gum [17,18], rice husks [19,20], and surface soil [21].

Activated carbon (AC) is typically used as an adsorbent for basic dyes [22,23]. It is widely employed due to its exceptionally high surface area (ranging from 500 to 1,500 $m^2 g^{-1}$), well-developed internal microporosity, and wide spectrum of surface functional groups. In this work, we used AC produced from orange, mandarin, and banana peels. These fruits are extensively grown in different parts of the world and in particular in the Mediterranean region. Moreover, they are usually available throughout the year. Because of the high consumption of these fruits, massive amounts of their peels are produced as waste, thereby causing great environmental and economic problems. Hence, we use these wastes as a low-cost precursor for the production of AC. The prepared AC was used as an alternative low-cost adsorbent for the removal of methylene blue (MB) (a basic and cationic dye) from aqueous solutions under varying conditions of initial concentration, pH, and carbon dosage.

2. Materials and methods

2.1. Materials

Fresh orange, mandarin, and banana peels were collected from local stores in Egypt. The collected peels were first washed by distilled water and dried by two methods. The first drying method involved the exposure of fruit peels to sun rays for 7–10 d until dry. The second drying method was heating the fruit peels in an oven at 130°C for 24 h. After drying, the peels were crushed and sieved with a 125-mm sieve. The AC was prepared by chemical activation of the dried fruit peels with concentrated H_2SO_4 (99.9% purity, BDH). The basic dye, MB, was used as the adsorbate in this investigation. It has the molecular formula $C_{16}H_{18}N_3SCl$ and a molecular weight of 319.85 g/mol. All other chemicals, such as sodium thiosulfate and iodine, were analytical grade.

2.2. Preparation of AC samples

A 40 g sample of the fruit peel powder was boiled with 120 mL of concentrated sulfuric acid (1:3 weight ratio) for 6 h in an air condenser system. After cooling, the final products were filtered and washed several times with a $NaHCO_3$ solution and distilled water until neutral pH was reached. After that, the resultant AC was dried at 110°C for 24 h and was subsequently weighed to determine the yield of the product. Finally, the AC was stored in tightly closed bottles. Table 1 shows the designations for the carbon samples and their treatment methods.

The yield of the final product was calculated using the initial weight of the dried fruit peels. The yield (%) was determined from the relation:

$$\text{Yield}\,(\%) = W_c/W_o \times 100 \quad (1)$$

where W_c is the final weight of the dry AC (g) and W_o is the weight of the fruit peels (g).

The prepared ACs were characterized by selected physical properties such as bulk density, average pore diameter, and surface area. This was accomplished using a mercury intrusion porosimeter (PoreSizer-9320, Micromeritics). Adsorption properties, including iodine number and point of zero charge (pH_{PZC}), were also determined. FTIR spectra of the chemically AC samples were obtained using a Fourier transform infrared spectrometer (BIO-RAD FTS-40).

2.3. Determination of iodine number

The iodine number is a widely used parameter for AC testing because of its simplicity and rapid assessment of quality. It has been established that the iodine number measures the accessibility of pores with dimensions ≥1.0 nm [24]. In addition, it gives an indication of the microporosity of the carbon samples [25]. Quality ACs are expected to have an iodine value equal to or higher than 900 mg/g. The iodine concentration was determined by a standard method [26] in which 10 mL of an iodine solution (0.1 N) in a conical flask was titrated with a sodium thiosulfate solution (0.1 N) in the presence of 2 drops of a 1 wt% starch solution indicator until the solution became colorless. Then, 0.05 g of AC was added to a conical flask containing 25 mL of the 0.1 N iodine solution; the mixture was shaken for 4 min and filtered. Ten milliliters of the filtrate was titrated with the standard sodium thiosulfate solution using 2 drops of starch solution as the indicator. The iodine number was then calculated using the following equation:

Table 1
Sample's designations and the treatment conditions

Sample designation	Fruit origin and activation conditions
OSS	Orange husks, sun dried and activated by sulfuric acid
OOS	Orange husks, oven dried and activated by sulfuric acid
MSS	Mandarin husks, sun dried and activated by sulfuric acid
MOS	Mandarin husks, oven dried and activated by sulfuric acid
BSS	Banana husks, sun dried and activated by sulfuric acid
BOS	Banana husks, oven dried and activated by sulfuric acid

$$\text{Iodine number } (1N) = \frac{(Vb - Vs)N\ (126.9)(15/10)}{M} \quad (2)$$

where V_b and V_s (mL) are volumes of the sodium thiosulfate solution required for the blank and sample titrations, respectively, N (mole /L) is the normality of the sodium thiosulfate solution, 126.9 is the atomic weight of iodine, and M (g) is the mass of the AC used.

2.4. Removal of MB

The adsorption of MB onto the AC samples was studied in a batch system. The effects of contact time, initial MB concentration, initial pH of the solution, and mass of the adsorbent were studied.

2.4.1. Effect of contact time

A 25 mL aliquot of the MB solution (1,000 mg/L) was agitated by shaking with 0.05 g of a carbon sample at 25°C for 15, 30, 60, 90, 120, 240, 360, and 1,140 min. At each time interval, the solid particles were removed by filtration. The remaining concentration of MB in the filtrate was measured using an UV–spectrophotometer (Specord 200) at 666 nm, corresponding to the maximum absorbency of MB; duplicated measurements were carried out and the average reading was recorded. The concentrations of the samples were determined using a linear regression equation obtained by plotting the calibration curve for MB over a range of concentrations. In samples containing high concentrations of MB, a dilution by 50 times was carried out to avoid errors. The adsorption capacity, q_{ad}, was calculated by applying Eq. (3):

$$q_{ad} = (C_0 - C_t) \times V/m \quad (3)$$

where q_{ad} is the adsorption capacity (mg/g) at time t, and C_0 and C_t are the concentrations (mg/L) of the MB solution before and after the adsorption process, respectively, V is the volume of the solution (L), and m is the mass of the adsorbent (g).

2.4.2. Effect of the initial MB concentration

A 50 mL aliquot of the MB solution with various initial concentrations (10, 20, 30, 40, 50, 70, 80, and 100 mg/L) was regularly stirred with 0.05 g of AC at an initial pH of 9 for 24 h at 25°C. After 24 h, the solid particles were removed by filtration, and the adsorption capacity was calculated using Eq. (3).

2.4.3. Effect of solution pH

A 0.05 g sample of AC was stirred with 25 mL of a MB solution possessing an initial concentration of 1,000 mg/L at various initial pH values (4–12) for 24 h at 25°C. After 24 h, the solid particles were removed by filtration and the adsorption capacity was calculated using Eq. (3).

2.4.4. Effect of adsorbent mass

The effect of the mass of the carbon samples on the removal capacity was studied using 50 mL of MB (C_0 = 110 mg/L at pH 9) with 0.05–0.5 g of carbon for 24 h at 25°C. The adsorption capacity was calculated by Eq. (3).

3. Results and discussion

3.1. Production yield

In producing commercial adsorbents, relatively high yields of the final products are expected. The production yields of the prepared activation carbon are shown in Table 2. These yields were in the range of 32–40% for fruits peels dried in sunlight and 25–30% for fruit peels dried in an oven at 130°C, before sulfuric acid treatment. The activation yield depends on the amount of carbon removed by binding with oxygen and hydrogen atoms; while the volatile content that evolved from the chemically AC depends on the pyrolysis temperature and the relative concentration of the solid particles to the activated reagent. The reason for the relatively high yield from sun drying compared with oven drying may be attributed to the

Table 2
Characterization of the ACs

Parameter	OSS	OOS	MSS	MOS	BSS	BOS
Yield %	40.2	30	36.8	28	32.4	25
Total pore area (m^2/g)	3.55	3.295	5.972	5.078	8.236	6.783
Average pore diameter (μm)	0.252	0.317	0.367	0.3977	0.1375	0.337
pH_{PZC}	6.5	7.5	8.3	7.2	8.4	7.3
Bulk density	1.816	1.348	1.392	1.783	0.851	0.898
Iodine number	540	–	750	–	1,060	1,012

evolution of a large portion of the volatile species in the oven. However, our yield is considered to be high, which may be attributed to a low burn-off and the more effective release of the volatile products as a result of intensifying the dehydration and elimination reactions that resulted in breaking the C–O–C and C–C bonds of the raw materials [27].

3.2. AC characterization

The surface characteristics of the prepared carbon samples were determined and are summarized in Table 2. According to the data reported in Table 2, the average pore diameters for all fruit peels are in the mesoporous range. However, this is not an indication of the absence of micropores [28]. Drying fruit peels in an oven before treatment with sulfuric acid decreased the total pore area and increased the average pore diameter compared with those of the sun-dried peels. Generally, the AC sample derived from banana peels showed a higher total pore area than that derived from mandarin peels, which is higher than that derived from orange peels. In addition, the banana peel samples (BSS, BOS) showed the lowest bulk densities and the highest iodine numbers (1,060, 10,120) for all investigated carbon samples. Because the iodine number measures the accessibility of pores with dimensions ≥1.0 nm [25,28], this reveals the formation of higher microporous fractions in BSS and BOS than those formed in the other fruit peel samples.

3.3. FTIR spectra

The Fourier transform infrared (FTIR) spectra of OOS, MOS, and BOS are shown in Fig. 1. The OOS spectrum displayed various stretching bands that are characterized as follows: A broad mixed stretching vibrational band from hydroxyl functional groups was observed at 3,426.9 cm^{-1}. The C=O stretching band from ketones, aldehydes, or carboxylic groups formed at 1,745.3 cm^{-1}. The C=C stretching in aromatic rings was present at 1,618.96 cm^{-1}. The C–O–C stretching band in ethers appeared at 1,126.2 cm^{-1}. The main functional groups present in OOS were carbonyl groups (such as ketone and quinone), ethers, and phenols. The MOS spectrum displayed the same stretching bands indicating that the same functional groups were present. The BOS spectrum showed an increase in the absorption band of hydroxyl functional groups at 3,426.9 cm^{-1} and the C=C stretching in aromatic rings at 1,618.96 cm^{-1}. Moreover, there is a reduction in the intensity of the C–O–C stretching band attributed to ethers at 1,126.2 cm^{-1}. The main functional groups present in the BOS sample were presumed to be phenols, carboxylic acids or carboxylic anhydrides and carbonyl groups. All of these functional groups are typical acidic functional groups, which favor the adsorption of cationic dyes such as MB.

3.4. Removal of MB

3.4.1. Effect of contact time and initial dye concentration on the uptake of MB

The effect of contact time on the adsorption capacity of different carbon samples for MB is shown in Fig. 2. The adsorbed amount of MB for all investigated carbon samples is increased by increasing the contact time. The adsorption reached equilibrium after approximately 1,140 min, after which nearly no more of the MB was removed from solution; this indicates a lack of active sites to which MB could bind. The adsorption capacity toward MB had the order of BOS > OOS > MOS and approximately 35–87% of the dye was adsorbed by the end of the removal process. The range of removal efficiencies could be attributed to variations in the texture, as well as different concentrations of the acidic functional groups present in the AC samples.

The adsorption of dyes at different initial concentrations gives information about the adsorption capacity of the adsorbent [29]. Hence, in this study, eight different initial concentrations of MB were studied to determine their effect on the adsorption capacity of carbon samples, and the results are presented in

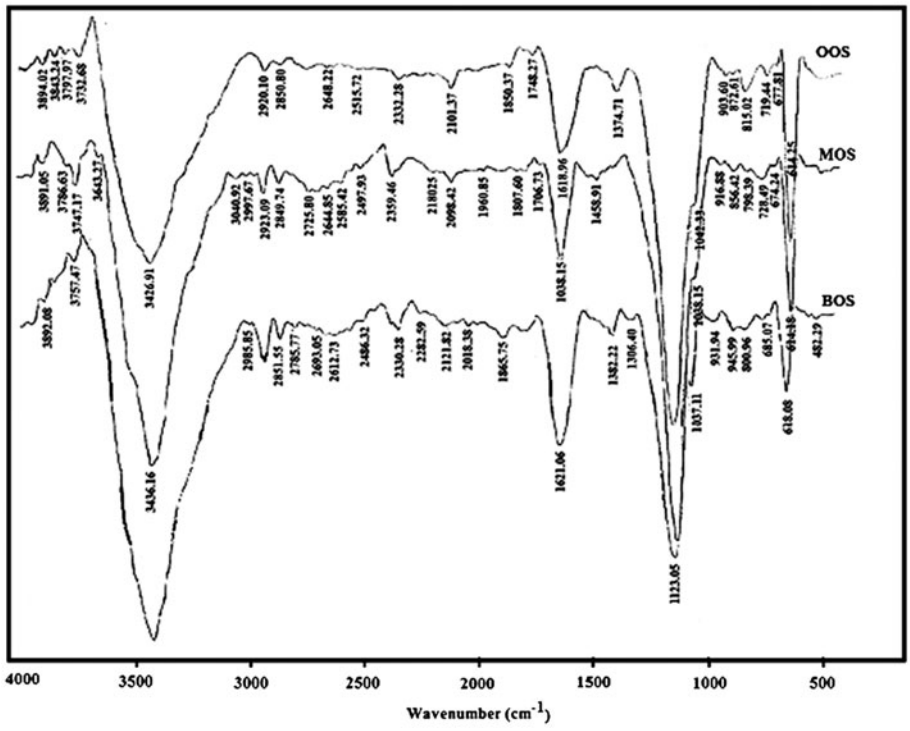

Fig. 1. FTIR of various AC samples.

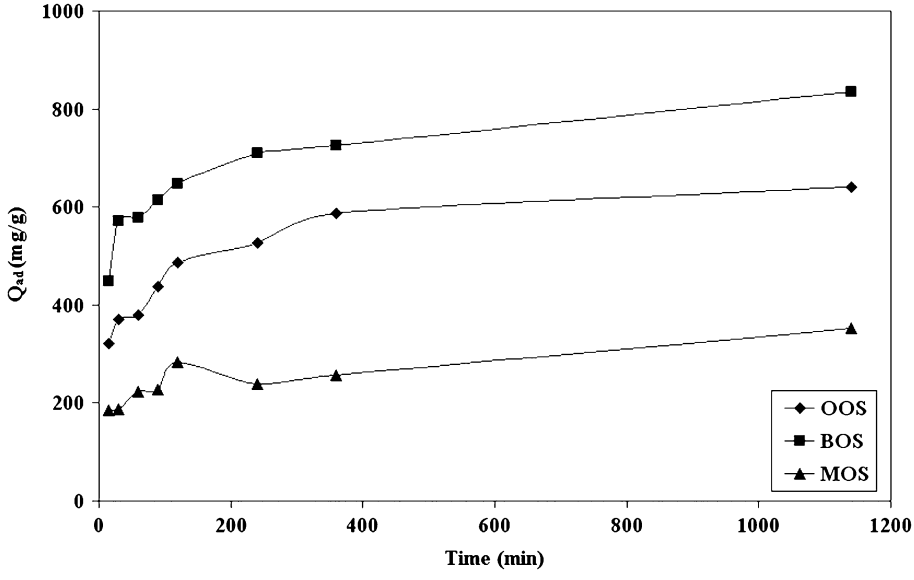

Fig. 2. Effect of contact time on the adsorption capacity of MB on AC V = 25 ml, C_0 = 1,000 mg/L, m = 0.05 g, pH 9.

Fig. 3. It can be concluded that at higher initial concentrations of MB, the removal of MB at equilibrium was high. A higher initial concentration provides a larger driving force to overcome the mass transfer resistance of MB from the aqueous phase to the solid carbon phase [29]. On the other hand, the BOS sample showed a higher adsorption capacity than those of the OOS and MOS samples.

3.4.2. Effect of pH values on adsorption

The pH of a dye solution plays an important role in the adsorption process, particularly on the adsorption capacity [30]. In general, the initial pH value may enhance or depress the dye uptake rate and is intercorrelated with changes in the adsorbent surface and dye chemistry [31].

Fig. 4 shows the effect of the initial pH of the MB solution (pH 4–12) on the adsorption capacity of the carbon samples derived from various fruit peels. It is noted that increasing pH in the range of 4–12 results in a continuous increase in the adsorption capacity, with a notable increase at pH 12—nearly all of the AC samples possessed equal adsorption capacities at pH 12. This indicates that the surface of the prepared carbon samples contains an excess of H^+ ions competing with the cationic MB for accessible adsorption sites, which reduces the amount adsorbed at low pH values. At alkaline pH, these acidic sites were deprotonated and the surface becomes negatively charged, which strongly attracts the cationic dye. Such an increase in the adsorption capacity at alkaline pH agrees with the values of pH_{PZC} determined for the prepared carbon samples, see Table 2. pH_{PZC} values were in the range of 7.3–8.6 indicating that the acidic sites on the prepared carbon surface were greater than the alkaline sites. A similar trend was observed for the adsorption of MB onto *Posidonia oceanica* (L.) fibers [32] and yellow passion fruit peel [33], and methyl violet onto sun flower seed hull [34].

The change in pH values due to the removal of MB by the BOS, MOS, and OOS samples is presented in Table 3. For the OOS and BOS samples, the pH of the solution shifted to neutral values when the initial pH value was less than 10. Whereas for the MOS sample, the shift was toward acidic pH. The three AC samples showed a final pH 9 when the initial solution was pH 12, and this explains why the three AC samples presented the same adsorption capacity at this initial pH.

3.4.3. Effect of adsorbent mass

Fig. 5 shows the effect of adsorbent mass on the amount of MB (mg/g) adsorbed. It is noted that the amount of MB adsorbed per gram of adsorbent decreases with increasing mass of the adsorbent. A 20-fold increase in modified mass resulted in a decrease in the adsorption capacity by 23- to 9.3-fold. Increasing the adsorbent mass reduces the unsaturation of the adsorption sites. Correspondingly, the number of such sites per unit mass is reduced resulting in a comparatively less adsorption. Additionally, increasing the adsorbent mass decreases the driving forces for adsorption (conc. of dye molecules/conc. of adsorption sites), which decreases the dye diffusion from solution into the adsorbent platelets. In addition, the overlapping of adsorption sites as a result of overcrowding of adsorbent particles may be another explanation [35,36].

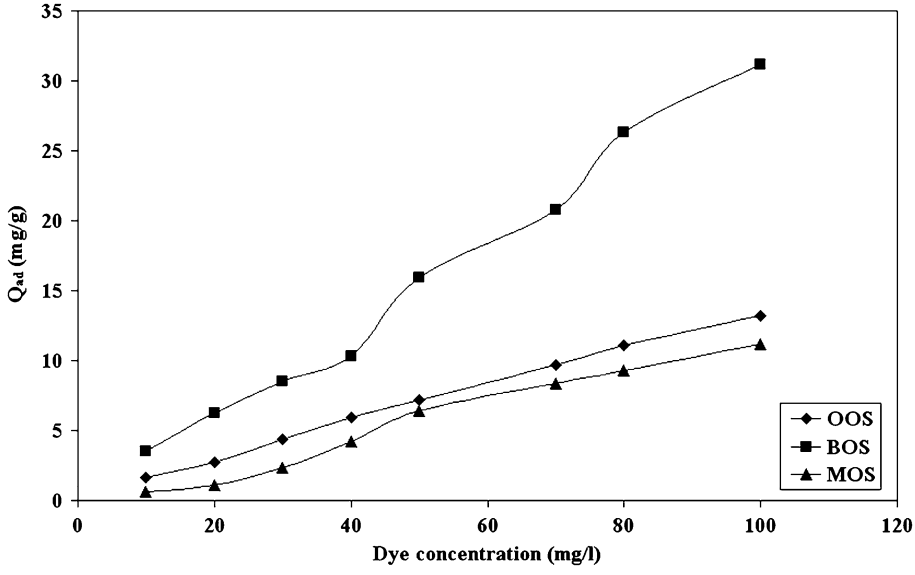

Fig. 3. Effect of initial dye concentration on the adsorption capacity of MB on AC V = 50 ml, pH 9, m = 0.05 g, contact time = 24 h.

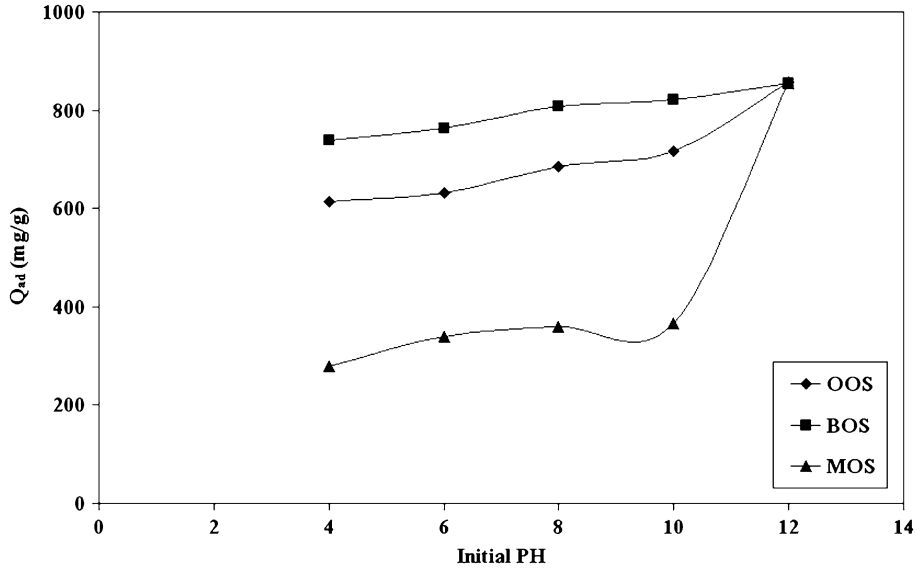

Fig. 4. Effect of pH on the adsorption capacity of MB on AC V = 25 ml, C_0 = 1,000 mg/L m = 0.05 g.

Table 3
Change of initial solution pH after MB adsorption

	Final pH		
Initial pH	OOS	MOS	BOS
4	7.12	3.73	6.5
6	7.5	4.3	7.4
8	7.4	4.1	7.1
10	7.5	5.1	7.45
12	9.35	9.14	9.35

3.5. Adsorption kinetics

To understand the process of adsorption, different kinetic models were used to investigate the experimental data.

The linear form of the pseudo-first-order kinetic model is expressed in Eq. (4):

$$\ln(q_e - q_t) = \ln q_e - k_1 t \quad (4)$$

where q_e is the concentration of MB adsorbed after equilibrium, q_t is the concentration of MB adsorbed in time t, and k_1 (min^{-1}) is the pseudo-first-order rate constant.

The pseudo-second-order rate equation in the linear form is expressed as:

$$t/q_t = 1/k_2 q_e^2 + t/q_e \quad (5)$$

where k_2 (g/mg/min) is the pseudo-second-order rate constant, which can be calculated from the intercept of the straight line obtained from plotting t/q_t vs. t. The initial sorption rate can be calculated using the relation:

$$K_i = k_2 Q_e^2 \quad (6)$$

The intraparticle diffusion model is an empirical model that assumes that the adsorption capacity varies with $t^{1/2}$ [37] (Eq. (7)):

$$q_t = K_d t^{1/2} + C \quad (7)$$

where K_d (mg/g $t^{-1/2}$) is the intraparticle diffusion rate parameter and C (mg/g) is a constant. Plotting q_t vs. $t^{1/2}$ gives a straight line when the diffusion model is valid. K_d and C were then determined from the slope and the intercept of the line. The value of C indicates the thickness of the boundary layer, and the larger the value of C, the greater the contribution of surface sorption in the rate limiting step.

The three models were tested with MB and various carbon samples. The best-fit model was determined by the linear correlation coefficient, R^2. The results are shown in Table 4. The pseudo-second-order plot and intraparticle diffusion models are represented in Figs. 6 and 7, respectively. According to the values of the correlation coefficients, OOS showed good fitting to the first-order rate equation (R^2 = 0.977), but the values of

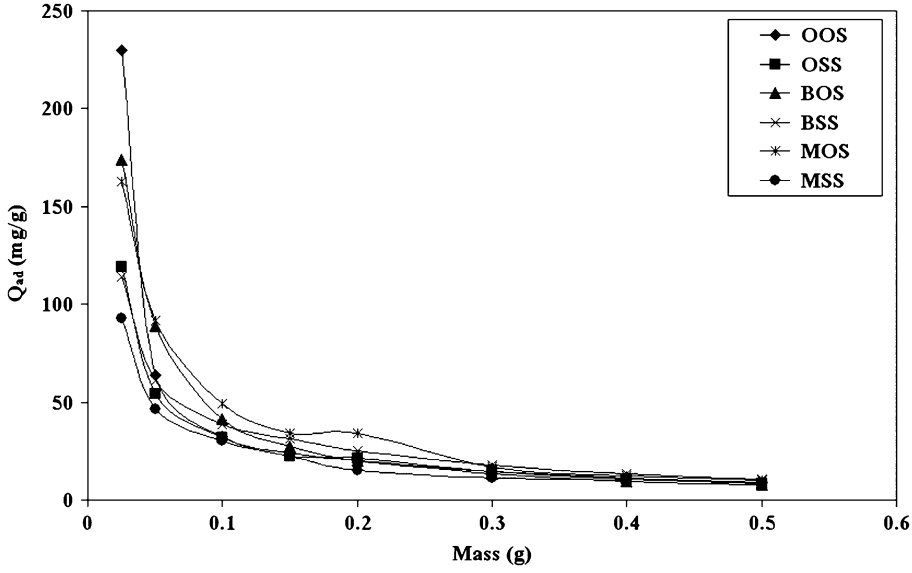

Fig. 5. Effect of mass on the adsorption capacity of MB on AC V = 50 ml, C_0 = 110 mg/L, pH 9.

$q_{e,cal}$ were much lower than those obtained experimentally ($q_{e,exp}$). However, the pseudo-second-order rate equation (R^2 = 0.998–0.992) showed better fitting to the experimental data for all samples than the first-order rate equation (R^2 = 0.977–0.405). In addition, the experimental q_e value ($q_{e,exp}$) and the calculated q_e value ($q_{e,cal}$) calculated from the pseudo-second-order kinetics model are closer to each other. Several researchers have reported that the pseudo-second-order kinetics model was the best-fit model for the adsorption of MB on other adsorbents, such as AC fiber, granular AC [22], banana leaf [38], and nanoparticles composites [36]. Table 4 gives a comparison of the maximum adsorption capacity of MB for various adsorbents [11,39–42].

The intraparticle diffusion model also showed good fitting to the experimental data (R^2 = 0.948–0.939), as shown in Fig. 7. The plots obtained for the three carbon samples present more than one linear region, which indicates that the intraparticle diffusion is not the only operative mechanism. This suggests that the adsorption of MB on the modified AC samples followed the second-order rate equation and was controlled by the diffusion of MB molecules from the bulk of the solution to the external surface and to the interior pores of the adsorbent [22,36] (Table 5).

3.6. Adsorption isotherms

To study how the molecules of MB interact with the adsorbent surface, the adsorption isotherms are used to analyze the experimental data. The most widely used isotherm equations are the Langmuir and Freundlich equations.

The Langmuir model was formulated for gas adsorption on homogeneous surfaces and was extended to adsorption from solution. In the Langmuir model, there is an active point on the surface of the adsorbent that is able to adsorb one molecule, indicating that the adsorbed layer is one molecule thick. The

Table 4
The maximum adsorption capacity of MB by different adsorbents

Adsorbent	Maximum adsorption capacity (mg/g)
Pineapple stem (PS) [11]	119.0
Activated carbon produced from flamboyant pods [22]	890
Waste activated sludge [23]	66.23
Garlic peel (GP) [24]	82.64 at 303 K, 123.45 at 313 K 142.86 at 323 K
Peanut hull [25]	90% of the initial dye concentration was removed
Banana leaf [26]	109.89

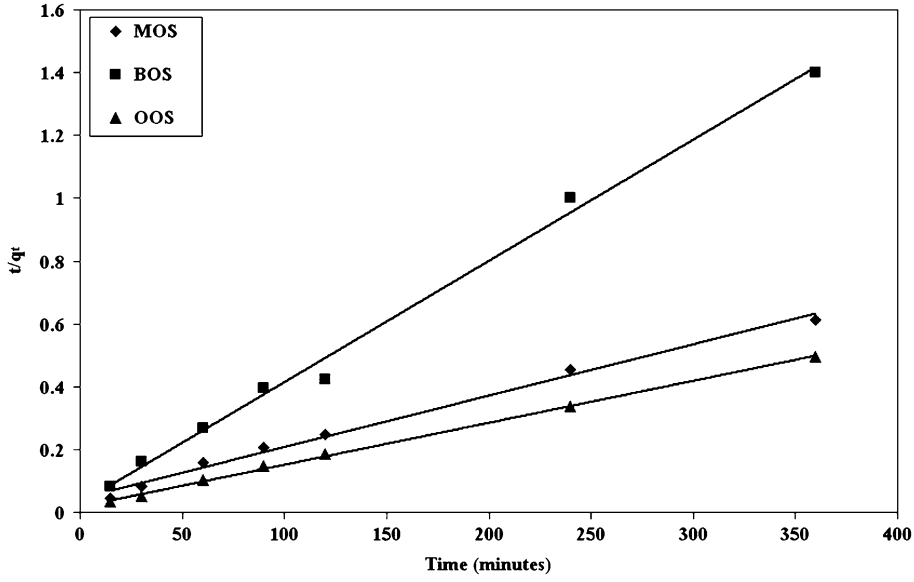

Fig. 6. Pseudo-second-order kinetics models.

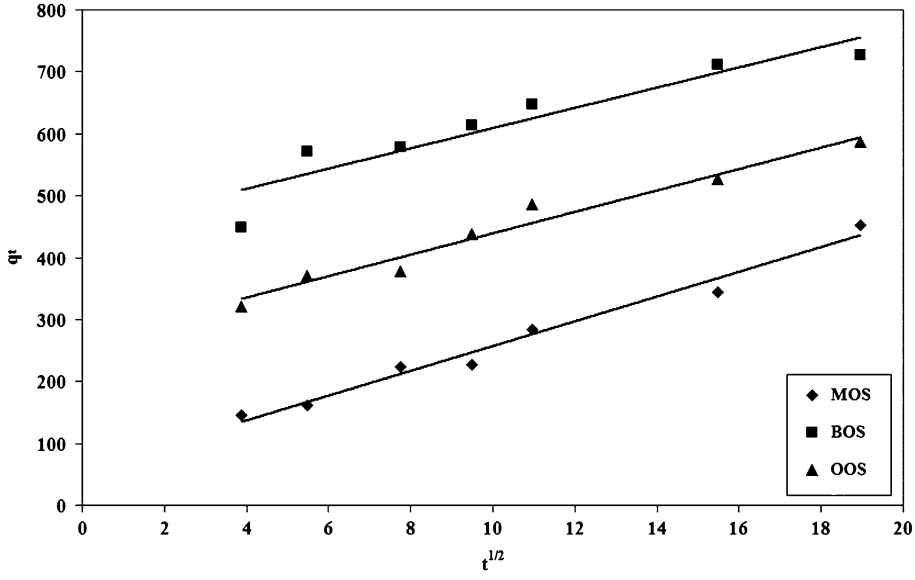

Fig. 7. Intraparticle diffusion model for MB on carbon samples.

model is characterized by a linear adsorption at low surface coverage, but becomes nonlinear as the adsorption sites approach saturation. It is expressed by the following equation (Eq. (8)):

$$C_e/q_e = 1/b\,q_m + C_e/q_m \quad (8)$$

where C_e (mg/L) is the equilibrium concentration, q_e (mg/g) is the amount adsorbed, q_m (mg/g) is the complete monolayer adsorption capacity, and b (L/mg) is the Langmuir constant.

The Freundlich isotherm is valid for nonlinear adsorption on heterogeneous surfaces, suggesting a multilayer adsorption on the adsorbent surfaces. Additionally, this empirical isotherm can be used for non-ideal sorption, in which the nonidentical adsorption sites are not always available.

The Freundlich equation is represented as follows:

Table 5
Adsorption parameters of various kinetic models

Model	Parameter	OOS	MOS	BOS
Pseudo-first-order rate equation	R^2	0.977	0.405	0.895
	k (min^{-1})	0.004	0.001	0.003
	$q_{e,exp}$ (mg/g)	641	352	835
	$q_{e,cal}$ (mg/g)	325	156	314
Pseudo-second-order rate equation	R^2	0.998	0.992	0.994
	k (g/mg min)	42×10^{-6}	51×10^{-6}	39×10^{-6}
	$q_{e,exp}$ (mg/g)	641	352	835
	$q_{e,cal}$ (mg/g)	690	400	810
	k_i	0.057	0.157	0.037
Intraparticle diffusion model	R^2	0.966	0.911	0.876
	K_{id} (g/mg $min^{1/2}$)	17.26	4.745	16.85
	C (mg/g)	266.4	180.3	455.9

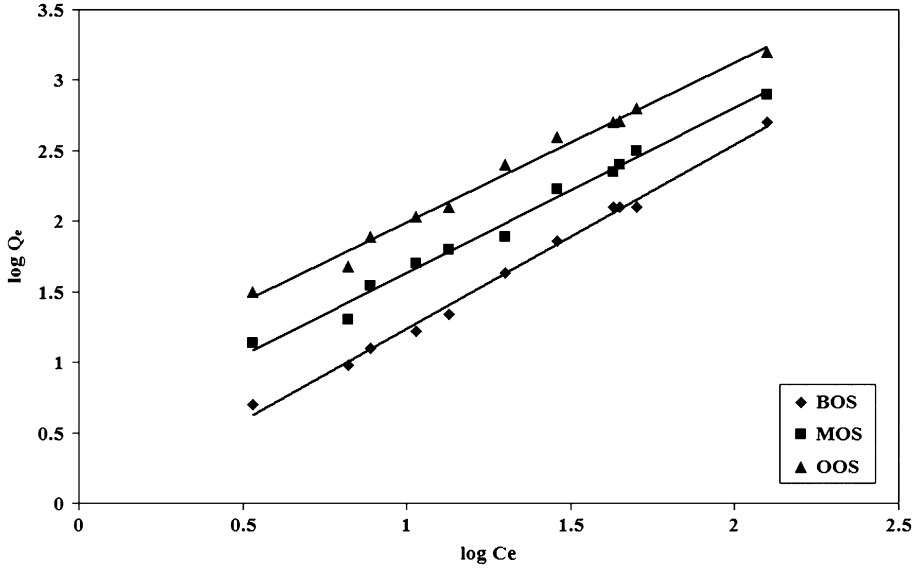

Fig. 8. Freundlich isotherm for MB on various carbon samples.

$$q_e = k C_e^{1/n} \quad (9)$$

and its linear form is

$$\log Q_{ad} = \log K_f + 1/n \log C_{eq}$$

where K_f and n are the Freundlich constants. The value $1/n$ is a measure of the adsorption intensity or surface heterogeneity, which may become more heterogeneous as $1/n$ approaches zero [43]. The value $1/n = 1$ indicates a linear adsorption; therefore, all sites are of equal adsorption energies. On the other hand, a value of $1/n < 1$ indicates a nonlinear isotherm.

In the literature, the adsorption of MB on various adsorbents has shown good fitting to both the Langmuir and Freundlich isotherms [44], while others have shown good fitting to either the Langmuir [22,38] or the Freundlich isotherm [41]. This variation may be related to the difference in the surface properties of the adsorbent and the types of function groups present on the surface, which affect the surface homogeneity or heterogeneity. Here, the data of various

Table 6
Isotherms study of adsorption of MB on ACs derived from various fruit peels

Isotherm	Parameter	OOS	MOS	BOS
Freundlich	K_f (mg/g)(L/mg)$^{-n}$	7.28	2.91	2.31
	$1/n$	1.13	1.168	1.3
	R^2	0.998	0.996	0.999
Langmuir	q_m (mg/g)	399	189	620
	K_L (L/mg)	0.286	0.121	0.317
	R^2	0.952	0.891	0.968

carbon samples are tested for the two adsorption isotherms. According to the R^2 values, the Freundlich isotherm (Fig. 8) showed good fitting to the experimental data than the Langmuir (not shown). Table 6 shows the Freundlich and Langmuir parameters. For the Freundlich isotherm, the value of $1/n = 1.3$–1.13 was obtained and indicates a linear adsorption where all sites are of equal adsorption energies.

4. Conclusions

ACs derived from orange, mandarin, and banana peels were prepared by boiling with sulfuric acid. The AC derived from banana peels showed the highest total pore area, the lowest bulk density, and the highest iodine number compared with all other studied carbon samples. According to the FTIR study, all carbon samples showed acidic functional groups on their surface, which is favorable for the adsorption of cationic dyes, such as MB. AC prepared from banana peels showed the highest removal efficiency compared with the other fruit peels. Adsorption isotherms were modeled with the Langmuir and Freundlich isotherms, and good fitting was observed for the Freundlich isotherm. The kinetic data were analyzed using pseudo-first, second-order, and intraparticle diffusion models, with good fitting to both the pseudo-second-order model and the diffusion model. Consequently, the prepared ACs could be used as an alternative low-cost adsorbent for dye removal.

Acknowledgment

The authors wish to express the deepest sense of gratitude to Prof Dr Gamal S. El-Shafei and Prof Dr Salah A. Abo-el-Enein for their valued help during the conduction of this work.

References

[1] H.M. Pinheiro, E. Touraud, O. Thomas, Aromatic amines from azo dye reduction: Status review with emphasis on direct UV spectrophotometric detection in textile industry wastewaters, Dyes Pigm. 61 (2004) 121–139.
[2] G. Crini, Non-conventional low-cost adsorbents for dye removal: A review, Bioresour. Technol. 97 (2006) 1061–1085.
[3] S. Chowdhury, R. Mishra, P. Saha, P. Kushwaha, Adsorption thermodynamics, kinetics and isosteric heat of adsorption of malachite green onto chemically modified rice husk, Desalination 265 (2011) 159–168.
[4] Z. Aksu, Application of biosorption for the removal of organic pollutants: A review, Process Biochem. 40 (2005) 997–1026.
[5] G. Annadurai, R. Juang, D. Lee, Use of cellulose based wastes for adsorption of dyes from aqueous solutions, J. Hazard. Mater. 92 (2002) 263–274.
[6] V.K. Gupta, Suhas, Application of low-cost adsorbents for dye removal—A review, J. Environ. Manage. 90 (2009) 2313–2342.
[7] Y.M. Slokar, A.M. Le Marechal, Methods of decoloration of textile wastewaters, Dyes Pigm. 37 (1998) 335–356.
[8] G.L. Dotto, L.A.A. Pinto, Adsorption of food dyes onto chitosan: Optimization process and kinetic, Carbohydr. Polym. 84 (2011) 231–238.
[9] M. Asgher, H.N. Bhatti, Evaluation of thermodynamics and effect of chemical treatments on sorption potential of Citrus waste biomass for removal of anionic dyes from aqueous solutions, Ecol. Eng. 38 (2012) 79–85.
[10] I.A.W. Tan, A.L. Ahmad, B.H. Hameed, Adsorption of basic dye on high-surface-area activated carbon prepared from coconut husk: Equilibrium, kinetic and thermodynamic studies, J. Hazard. Mater. 154 (2008) 337–346.
[11] B.H. Hameed, Spent tea leaves: A new non-conventional and low-cost adsorbent for removal of basic dye from aqueous solutions, J. Hazard. Mater. 161 (2009) 753–759.
[12] P. Janos, H. Buchtov´a, M. R´yznarov´a, Sorption of dyes from aqueous solutions onto fly ash, Water Res. 37 (2003) 4938–4944.
[13] M. Visa, M. Nacu, Comparative heavy metals and dyes removal efficiency on fly ash and wood ash, Environ. Eng. Manage. J. 10 (2011) 1407–1410.
[14] M. Visa, L. Andronic, D. Lucaci, A. Duta, Concurrent dyes adsorption and photo-degradation on fly ash based substrates, Adsorption 17 (2011) 101–108.
[15] W. Shaobin, Y. Boyjoo, A. Choueib, Z.H. Zhu, Removal of dyes from aqueous solution using fly ash and red mud, Water Res. 39 (2005) 129–138.
[16] R. Gong, M. Li, C. Yang, Y. Sun, J. Chen, Removal of cationic dyes from aqueous solution by adsorption on peanut hull, J. Hazard. Mater. 121 (2005) 247–250.
[17] F.F. Simas, P.A.J. Gorin, R. Wagner, G.L. Sassaki, A. Bonkerner, M. Iacomini, Comparison of structure of gum exudate polysaccharides from the trunk and fruit of the peach tree (*Prunus persica*), Carbohydr. Polym. 71 (2008) 218–228.

[18] Y. Xie, S. Ren, Study on fuzzy comprehensive evaluation in optimization for the matrix of peach-gelatin-based microcapsule, J. Food Sci. Technol. 9 (2008) 112–116.
[19] W. Zou, K. Li, H. Bai, X. Shi, R. Han, Enhanced cationic dyes removal from aqueous solution by oxalic acid modified rice husk, J. Chem. Eng. Data 56 (2011) 1882–1891.
[20] V. Vadivelan, K.V. Kumar, Equilibrium, kinetics, mechanism, and process design for the sorption of methylene blue onto rice husk, J. Colloid Interface Sci. 286 (2005) 90–100.
[21] B.C. Qu, J.T. Zhou, X.M. Xiang, C.L. Zheng, H.X. Zhao, X.B. Zhou, Adsorption behavior of Azo Dye C. I. Acid Red 14 in aqueous solution on surface soils, J. Environ. Sci. 20 (2008) 704–709.
[22] H.A. AL-Aoh, R. Yahya, M.J. Maah, M.R. Bin Abas, Adsorption of methylene blue on activated carbon fiber prepared from coconut husk: Isotherm, kinetics and thermodynamics studies, Desalin. Water Treat. 52 (2014) 6720–6732.
[23] R. Lakshmipathy, N.C. Sarada, Methylene blue adsorption onto native watermelon rind: Batch and fixed bed column studies, Desalalin. Water Treat. (2015) 1–14, doi: 10.1080/19443994.2015.1040462.
[24] N.M. Haimour, S. Emeish, Utilization of date stones for production of activated carbon using phosphoric acid, Waste Manage. 26 (2006) 651–660.
[25] K. Sun, J.C. Jiang, Preparation and characterization of activated carbon from rubber seed shell by physical activation with steam, Biomass Bioenergy 34 (2010) 539–544.
[26] ASTM, D4607-94, Standard Test Method for Determination of Iodine Number of Activated Carbon, American Society for Testing and Materials (2006) 1–5.
[27] A.H. Basta, V. Fierro, H. El-Saied, A. Celzard, 2-Steps KOH activation of rice straw: An efficient method for preparing high-performance activated carbons, Bioresour. Technol. 100 (2009) 3941–3947.
[28] K.S.W. Sing, The use of physisorption for the characterization of microporous carbons, Carbon 27 (1989) 5–11.
[29] G.S. ElShafei, I.N. Nasr, A.S.M. Hassan, S.G.M. Mohammad, Kinetics and thermodynamics of adsorption of cadusafos on soils, J. Hazard. Mater. 172 (2009) 1608–1616.
[30] B. Yasemin, A. Haluk, A kinetics and thermodynamics study of methylene blue adsorption on wheat shells, Desalination 194 (2006) 259–267.
[31] K.Y. Foo, B.H. Hameed, An overview of dye removal via activated carbon adsorption process, Desalin. Water Treat. 19 (2010) 255–274.
[32] M.C. Ncibi, B. Mahjoub, M. Seffen, Kinetic and equilibrium studies of methylene blue biosorption by *Posidonia oceanica* (L.) fibres, J. Hazard. Mater. 139 (2007) 280–285.
[33] F.A. Pavan, A.C. Mazzocato, Y. Gushikem, Removal of methylene blue dye from aqueous solutions by adsorption using yellow passion fruit peel as adsorbent, Bioresour. Technol. 99 (2008) 3162–3165.
[34] B.H. Hameed, Equilibrium and kinetic studies of methyl violet sorption by agricultural waste, J. Hazard. Mater. 154 (2008) 204–212.
[35] C. Namasivayam, D. Prabha, M. Kumutha, Removal of direct red and acid brilliant blue by adsorption on to banana pith, Bioresour. Technol. 64 (1998) 77–79.
[36] F.S. Hashem, Removal of methylene blue by magnetite-covered bentonite nanoparticles, Eur. Chem. Bull. 2 (2013) 524–529.
[37] W.J. Weber, J.C. Morris, Advances in water pollution research: Removal of biologically resistant pollutant from waste water by adsorption, International Conference on Water Pollution Symposium, vol. 2, Oxford, Pergamon, 1969, pp. 231–266.
[38] R.R. Krishni, K.Y. Foo, B.H. Hameed, Adsorptive removal of methylene blue using the natural adsorbent-banana leaves, Desalin. Water Treat. 52 (2014) 6104–6112.
[39] A.M.M. Vargas, A.L. Cazetta, M.H. Kunita, T.L. Silva, V.C. Almeida, Adsorption of methylene blue on activated carbon produced from flamboyant pods (*Delonix regia*): Study of adsorption isotherms and kinetic models, Chem. Eng. J. 168 (2011) 722–730.
[40] K. Gobi, M.D. Mashitah, V.M. Vadivelu, Adsorptive removal of Methylene Blue using novel adsorbent from palm oil mill effluent waste activated sludge: Equilibrium, thermodynamics and kinetic studies, Chem. Eng. J. 171 (2011) 1246–1252.
[41] B.H. Hameed, A.A. Ahmad, Batch adsorption of methylene blue from aqueous solution by garlic peel, an agricultural waste biomass, J. Hazard. Mater. 164 (2009) 870–875.
[42] R. Gong, Y. Sun, J. Chen, H. Liu, C. Yang, Effect of chemical modification on dye adsorption capacity of peanut hull, Dyes Pigm. 67 (2005) 175–181.
[43] F. Haghseresht, G.Q. Lu, Adsorption characteristics of phenolic compounds onto coal-reject-derived adsorbents, Energy Fuels 12 (1998) 1100–1107.
[44] J. Zolgharnein, M. Bagtash, Hybrid central composite design Optimization for removal of Methylene blue by Acer tree leaves: Characterization of adsorption, Desalin. Water Treat. 54 (2015) 2601–2610.